Boride-based nano-laminates with MAX-phase-like behaviour

Rainer Telle[a],*, Ai Momozawa[a], Denis Music[b], Jochen M. Schneider[b]

[a]Institut fuer Gesteinshuettenkunde (Mineral Engineering), Chair of Ceramics and Refractory Materials, RWTH Aachen, Mauerstrasse 5,
D-52056 Aachen, Germany
[b]Materials Chemistry, RWTH Aachen, Germany

Abstract

MAX-phases being usually composed of transition metals, group A elements and carbon/nitrogen are considered interesting materials for many applications because of their tremendous bulk modulus, "reversible" plasticity, and machinability. This is mainly due to their unique kind of bonding comprising covalent, ionic as well as metallic bonds providing "easy" planes of rupture and deformability due to the layered crystal structures.

In transition metal boride systems, similar types of bonding are available. In particular the W_2B_5-structure type and its stacking variations allow the synthesis of strongly layered crystal structures exhibiting unique delamination phenomena.

The paper presents ab initio calculations showing the similarities of bonding between the ternary carbides and the corresponding ternary or quaternary borides. Formation of boride-based nano-laminates from auxiliary liquid phases, from the melt as well as during sintering and precipitation from supersaturated solid solutions will be discussed by means of SEM and TEM studies. The role of impurities weakening the interlayer bonding will be addressed in particular. The pronounced cleavage parallel to the basal plane gives rise for crack deflection and pull-out mechanisms if the laminates are dispersed in brittle matrices such as boron carbide, silicon carbide or other transition metal borides.
© 2006 Elsevier Inc. All rights reserved.

1. Introduction

"MAX-phase" is a term usually assigned to ternary metal carbides of the general formula $M_{n+1}AX_n$ with $n = 1, 2$, or 3, where M is a transition metal such as Ti, Zr, Hf, Nb, Ta, Mo, and others, A is mostly a IIIA and IVA group metal such as Al, Ga, Ge, Sn, Pb, In, but also As, P, and others, whereas X is either C or N.

The peculiar characteristic of these ternary compounds is their layered structure, which is composed of alternating hexagonal planar networks of A-group elements and $M_{n+1}X_n$ polyhedra—mostly octahedral with X in the centre—which are arranged to edge-bonded planar layers as well. The resulting crystal structure belongs to space group $P6_3/mmc$ and possesses a rather weak bonding between the A-layers and the $M_{n+1}X_n$-layers. Ternary

phases have been described, first by Jeitschko and Nowotny [1], Wolfsgruber et al. [2], Nowotny [3], later by Pietzka and Schuster [4] and others in detail, but only Barsoum paid special attention to their mechanical peculiarities, e.g. [5–8]; he regarded these phases as a novel kind of material named "nano-laminates".

MAX-phases appear in three major classes of chemical stoichiometry, (i) the so-called 211 class, of which Ti_2AlC is one of the more interesting members but which comprises more than 50 known compounds, (ii) the 321 class with, among others, $Ti_3(Al,Si)C_2$, and (iii) the 413 class with Ti_4AlN_4 as the only member. According to the crystal structure, these compounds contain metallic bonds among the M atoms, but also some portions of covalent bonding owing to the presence of carbon and nitrogen, which provide relatively high stiffness, low thermal expansion coefficients, excellent thermal and electric conductivity similarly to other transition metal carbides and nitrides such as TiC and TiN. Owing to their pronounced

*Corresponding author. Fax: +49 241 809 2226.
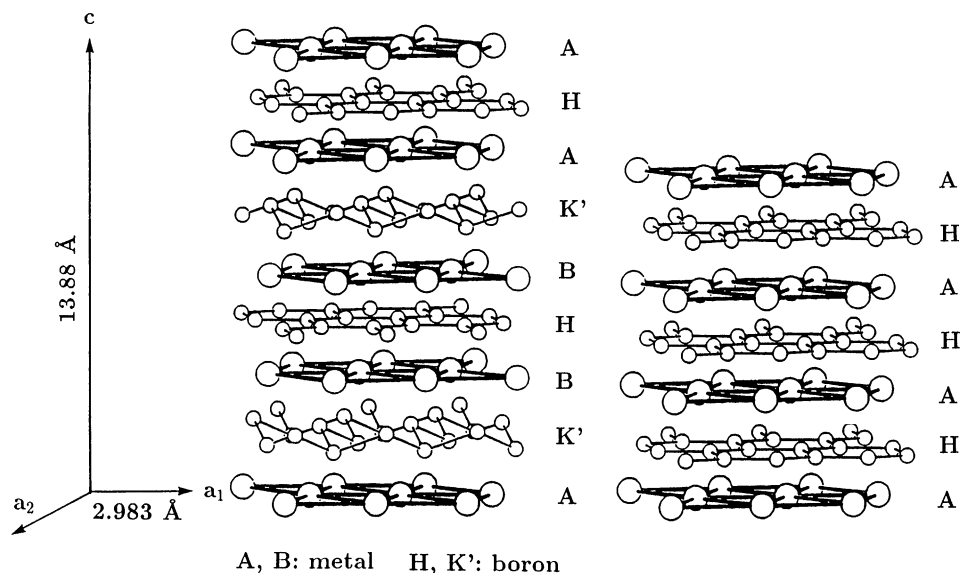E-mail address: telle@ghi.rwth-aachen.de (R. Telle).

Fig. 1. Layered structures of AB$_2$-type borides: Left: W$_2$B$_5$ type; right: AlB$_2$ type. Note the difference in stacking sequence of metal layers.

anisotropic structure, however, they are claimed to be relatively soft but readily machinable and "damage tolerant" as proposed by Barsoum et al. [9]. In particular, they seem to be tolerant to compressive stresses, which was recently explained by an easy formation of kink bands within the basal planes while being sheared [10].

Layered structures exhibiting strongly anisotropic bonding are also known from borides based on the AlB$_2$ structure, which belong to space group $P6/mmm$ and consist of alternating stacks of basal centred hexagonal metal layers (Al, Ti, Zr, Ta, and other transition metals), and boron layers (Fig. 1). Similarly to carbide and nitride-based MAX-phases, these materials have metallic bonding in the intermetallic layers but much stronger covalent bonding within the boron network, which is responsible for the extraordinarily high melting points, hardness and stiffness of this group of materials. In addition, owing to a lack of electrons in the boron sublattice, ionic bonds are generated between the layers since the metal sublattice donates some electrons to the boron sublattice and thus becomes slightly positively charged [11]. These rather weak ionic bonds were thought to be responsible for the significant anisotropy of thermal expansion [12], Young's modulus, hardness and both thermal and electric conductivity. The type of atomic bonding and, consequently, the anisotropy of the thermo-physical properties may be considerably changed if the structural layers are chemically modified [12]. Taking into account previous observations [14] it is worthwhile looking at β-WB, W$_2$B$_5$, and Mo$_2$B$_5$-type structures for "MAX-phase like" behaviour, in particular, since these phases may be used for the reinforcement of other ceramic matrix phases which are chemically compatible. It should be noted that in this paper the terms "W$_2$B$_5$" and "Mo$_2$B$_5$" refer to structure types and not to chemical composition, which should be referred to as WB$_{2-x}$ and MoB$_{2-x}$, respectively.

2. Experimental and theoretical methods

In order to investigate chemical bonding between metal and boron sublattices ab initio calculations were carried out with the Vienna ab initio software package (VASP) [15] applying the density functional theory [16]. The VASP program works on the plane wave basis with a generalised-gradient approach. The electron interaction is simulated by projector-augmented waves. The integration in the Brillouin zone is done on special k-points. The convergence criterion for the total energy was 0.01 meV within a 400 eV cut-off. Spin polarisation was disregarded since the energy difference between paramagnetic and spin polarised state was within 22 meV/atom. All structures were relaxed with respect to atomic positions, lattice parameters a, i.e. Wigner-Seitz primitive cell volume, and the c/a ratio. Furthermore, electron density distributions for all configurations were calculated.

Materials synthesis was carried out by (i) powder route and (ii) auxiliary bath method. The starting powders used in the following experiments were supplied by H.C. Starck, Goslar, Germany. Powders of TiB$_2$ (H.C. Starck Grade A, 0.13 wt% Fe, 0.29 wt% C, 0.08 wt% N), CrB$_2$ and W$_2$B$_5$ (H.C. Starck, 12.38 wt% B, 87.01 wt% B, 0.29 wt% C, 0.19 wt% O, 0.01 wt% Fe) were attrition-milled in the ratio 40:50:10 mol% with Co-bonded hard metal balls in isopropanol. The dried powder was uniaxially prepressed into cylinders and hot pressed for 0.5 h at 1800 °C under 1 atm Ar pressure with 50 MPa. The specimens were annealed at 2000–2200 °C for 8 h to homogenise the solid solution of (Ti,W,Cr)B$_2$. In a subsequent step the specimens were annealed without pressure at 1600 °C for 8 h to precipitate the W$_2$B$_5$-type structure of WB$_2$. All annealing treatment was performed under 1 atm Ar.

The samples were characterised by XRD (Philips PW3020), SEM (LEO 440i with Oxford EDX System Link

Isis). For TEM studies the samples were thinned by cutting, polishing, dimpling, and ion beam milling. For EFTEM investigations a Philips CM30ST/STEM and the Philips CM300UTFEG, both operating at 300 kV, were used and equipped with a post-column imaging electron energy filter (Gatan imaging filter (GIF)).

In order to obtain large crystals without matrix phase the auxiliary bath method was applied. W powder (Fulka, 99,8%) and B powder (Fulka, 98.5%, res. O, N, C) were mixed together with metallic Al flakes (Merck-Schuchardt, 0.14 wt% Fe, 0.01 wt% N, 0.2 wt% O) and heated to 1350 °C in an alumina crucible. After soaking for 10 h the crucible was cooled down at a rate of 50 K/h. The aluminum was dissolved in diluted HCl in order to recover the crystals. The same procedure was applied to a powder blend of 20 wt% W_2B_5, 10 wt% TiB_2, and 70 wt% Si (H.C. Starck, Goslar, 0.22 wt% Fe, 0.05 wt% Al, 0.6 wt% O). Dissolution of powder in the melt occurred at 1800 °C during 1 h in Ar atmosphere. The cooling rate was 5 K/min. In this case the polished sections were prepared from the crystals imbedded in the silicon matrix and documented in polarisation reflected light microscopy. In order to enhance the contrast the sections were coated with platinum oxide by means of a plasma-discharge device.

Another kind of large crystals were prepared by melting W_2B_5 powder at 2400 °C in a hexagonal boron nitride-coated graphite crucible in Ar atmosphere, which allowed crystal growth during uncontrolled cooling.

3. Results

3.1. Observations on individual crystals

Both the auxiliary bath method and melt-derived crystal growth yielded large hexagonal crystals of several millimetres' diameter (Fig. 2). The melt-derived crystals grew in an orientation parallel to the bottom of the crucible. Anisotropic sections could thus be obtained from these samples as well. Figs. 3 and 4 show the typical bending behaviour which resembles that reported from MAX-phases.

In order to understand the behaviour of the individual crystals, polished cross sections perpendicular to the basal plane were analysed by SEM/EDX and TEM. For the crystals grown from Si melt the phenomenon of cleaving was observed without an external mechanical load. A detailed analysis reveals that the crystals contain an average of 32.9±0.1 at% W and 0.4±0.1 at% Ti. The accumulation of impurities and dopants such as Al, Fe, Ti, and Si on the basal planes is thought to weaken the inter-sublattice forces. Fig. 5 yields evidence of impurity segregation due to the light grey contrast indicating the area depleted.

HR-TEM studies prove the existence of foreign metals on basal planes in the case of polycrystalline CrB_2-doped B_4C–TiB_2–W_2B_5 composites [13] giving evidence that Cr was in this case incorporated in the metal layer of W_2B_5
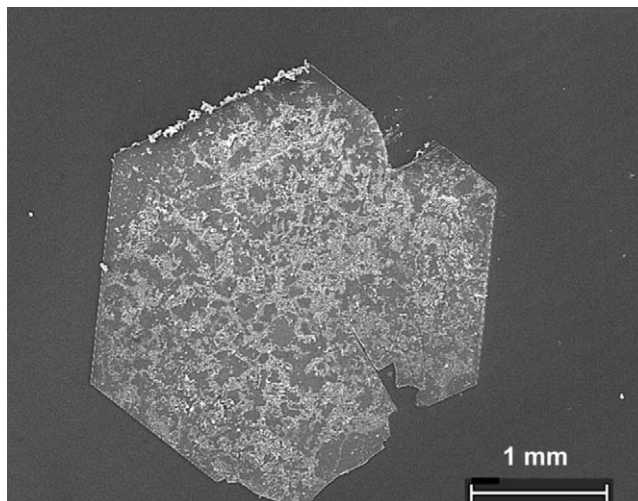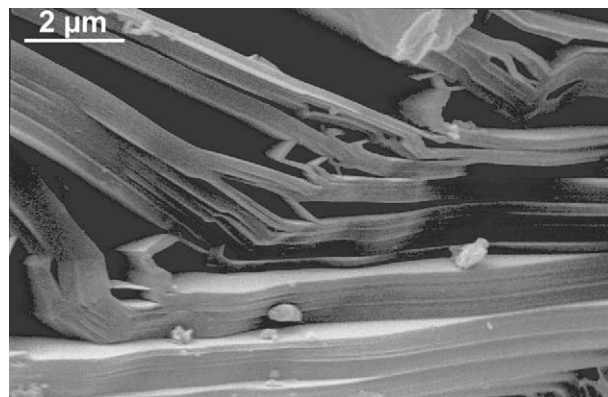

Fig. 2. W_2B_5 crystal grown in Al melt.

Fig. 3. W_2B_5 crystal grown from melt showing severe delamination.
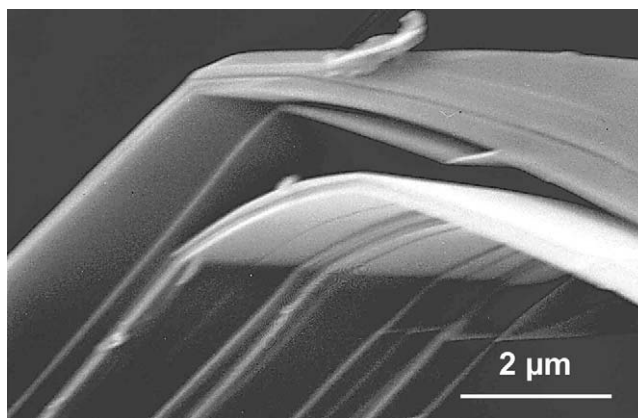

Fig. 4. Kink band formation in W_2B_5 crystal.

giving rise to a change from $P6_3/mmc$ to $P6/mmm$ (AlB_2-type) symmetry. This is realised by leaving out the K′-layer of the boron sublattice and creating an AHA-sequence instead (Fig. 6). This phenomenon may either be the consequence of an inward-diffusion of foreign metal atoms
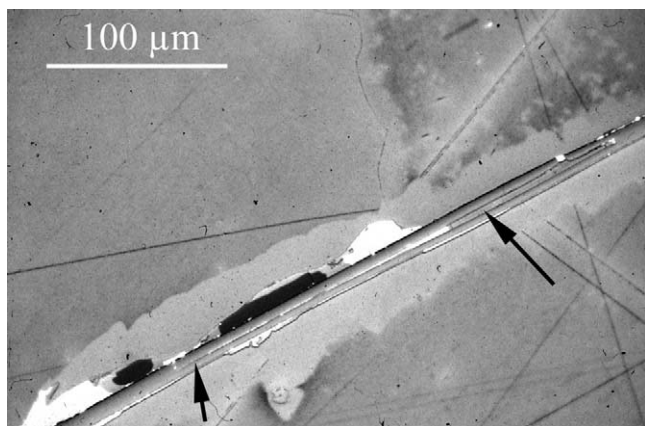
Fig. 5. W_2B_5 grown from Si melt. Note the cleavage effect (arrows) and the depletion of liquid from impurities.
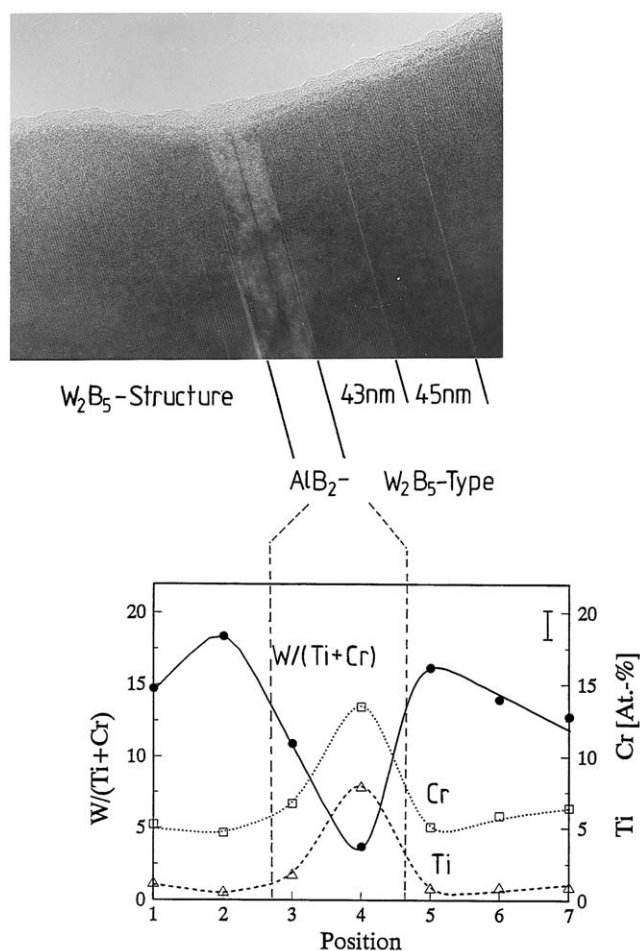

Fig. 6. STEM/EDS-measurement across an AlB_2-type stacking sequence in W_2B_5 crystals. Note the enrichment of CrB_2 and TiB_2 along the basal plane [13].

generating a progressive lateral growth of a stacking fault (Fig. 7) or may be due to prevention of further grain growth into *c*-direction during sintering or precipitation from liquid phases (Fig. 5).

3.2. Observations on ceramics

Because the weak bonding between the particular layers gave rise to a paper-like bending behaviour it was tested whether this effect may be used to reinforce ceramic matrices such as boron carbide, silicon carbide, or other AlB_2-type transition metal borides. As we know from fibre reinforcement of ceramics, appropriate conditioning of the fibre/matrix interface is a prerequisite for efficient crack deflection or particle pull-out. This is why fibres are usually coated either by CVD techniques or briefly oxidised in order to generate a thin film to "lubricate" the grain boundaries.

As described in previous work [18,19] samples of B_4C–TiB_2–W_2B_5 composites were prepared by reaction hot pressing starting from a reactive powder mix of B_4C, TiB_2, B, and WC where B and WC forms W_2B_5 or in the presence of TiB_2 a $(Ti,W)B_2$ solid solution. Hot-pressing at $1800\,^\circ C$ resulted in the euhedral growth of W_2B_5 platelets but the peculiar fracture characteristics were not observed in the composite owing to the small particle size and the weak interfacial strength between W_2B_5 and B_4C matrix. Crack deflection along the interface is observed instead (Figs. 8 and 9).

In the case of SiC matrix composites, where W_2B_5 was grown in situ by reaction between WC and elemental B, the crack tends to proceed *inside* the crystal parallel to the basal plane indicating that this path requires less fracture energy than the one along the interface to the matrix material (Fig. 10). This, however, only happens under optimum conditions. Crack bridging by elastically deformed W_2B_5 until transverse rupture occurs is also a common feature in SiC–W_2B_5 composites (Fig. 11).

In transition metal boride ceramics prepared from TiB_2–W_2B_5–CrB_2 powder blends, some particular precipitates were observed which may also act as reinforcing compounds [14,20]. After generating a homogeneous AlB_2-type $(Ti, W, Cr)B_2$ solid solution during annealing at $>2000\,^\circ C$, precipitation of W-depleted spinodal solid solution, euhedral W_2B_5 platelets heterogeneously nucleated at the grain boundaries, and epitaxial Cr-stabilised β-WB-type $TiWB_2$ laminates are observed (Fig. 12). As mentioned before, the reinforcing role of the W_2B_5 particles is well established. Surprisingly, the β-WB-type precipitates proved to interact with cracks as well although their thickness ranges from 5 to 20 nm only but extending to 10–100 µm (Fig. 13).

3.3. Quantum mechanical calculations

Ab initio calculations of the W_2B_5 structure reveal that boron forms covalent-ionic chains interleaved with tungsten and that the electron density between the tungsten layers and the K'-layers of boron is low and, therefore, the bond strength is weak (Fig. 14). Similar calculations have been carried out on the structurally related compounds Mo_2B_5, Re_2B_5, and Os_2B_5 based on the structural data of [21]. This rather weak bonding may easily explain the sensitivity
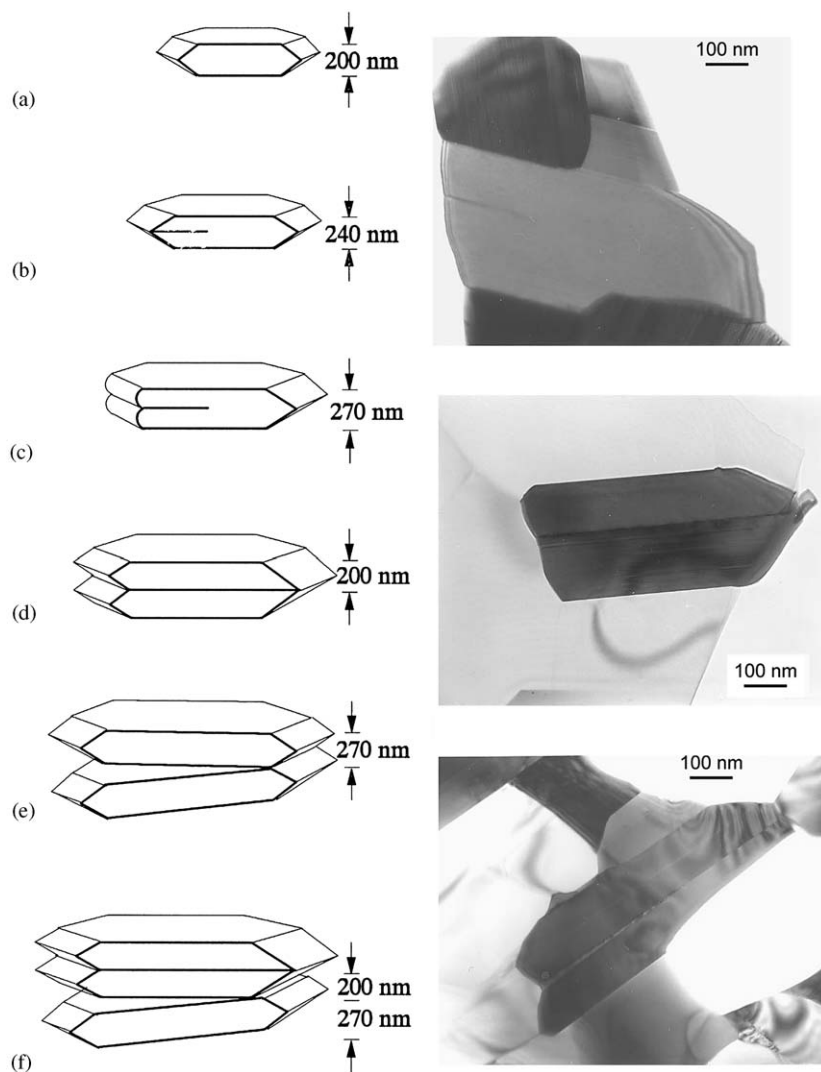
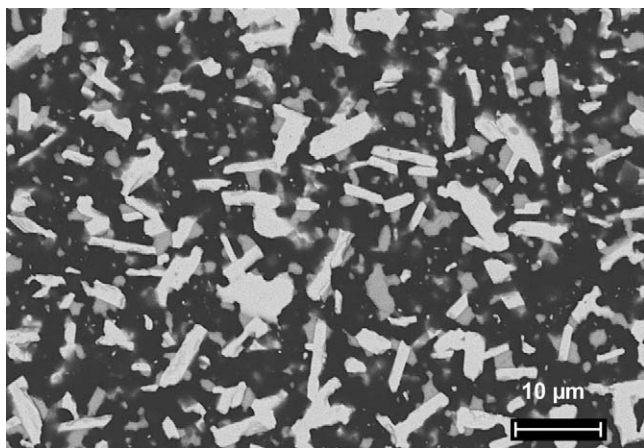Fig. 7. Progressing cleavage of W_2B_5 crystal depending on thickness [17].

Fig. 8. Reaction hot-pressed B_4C–TiB_2–W_2B_5 composite. Note the plate-shaped growth of W_2B_5 (bright imaged).

Fig. 9. Fracture surface of composite of Fig. 8. Note the smooth crack path along the boundary between W_2B_5 and B_4C matrix.

of the crystals for a delamination along the basal plane in particular if these "weak" planes accommodate foreign species such as ch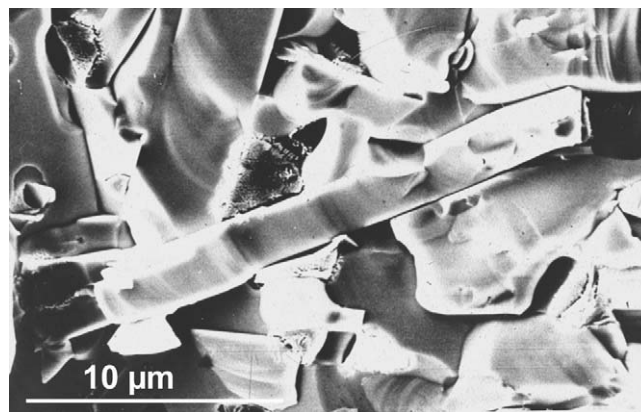romium or, in other cases, carbon or nitrogen. Moreover, the bonding in the $(11\bar{2}0)$ planes in the here-presented borides is rather similar to the bonding in the $(11\bar{2}0)$ planes in the MAX-phases [22]. The alternating
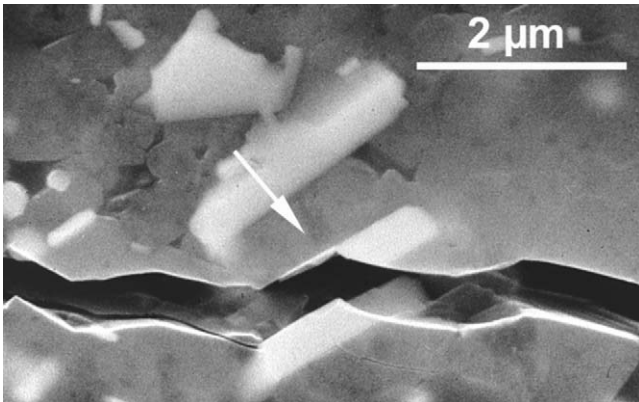
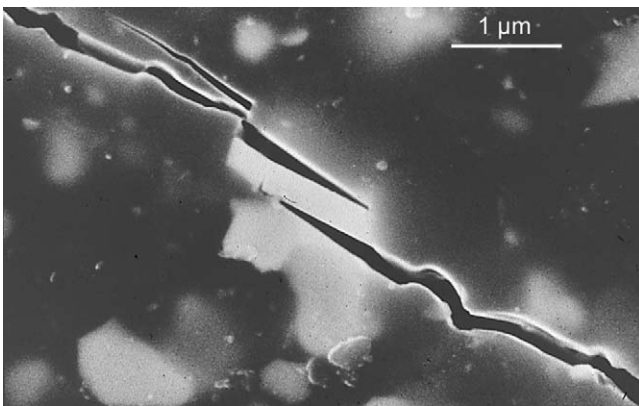Fig. 10. Crack deflection *inside* W_2B_5 parallel to interface to matrix.

Fig. 11. Crack bridging in SiC–W_2B_5.

stacks of metal and boron layers in these borides (see Fig. 1) correspond to the alternating stacks of A-elements and carbides (or nitrides) in the MAX-phases. Barsoum and coworkers have categorised the MAX-phases as a new class of solids [23], exhibiting a combination of metallic and ceramic properties. Therefore, according to similarities in the bond, it is reasonable to assume that W_2B_5-based compounds exhibit similar properties.
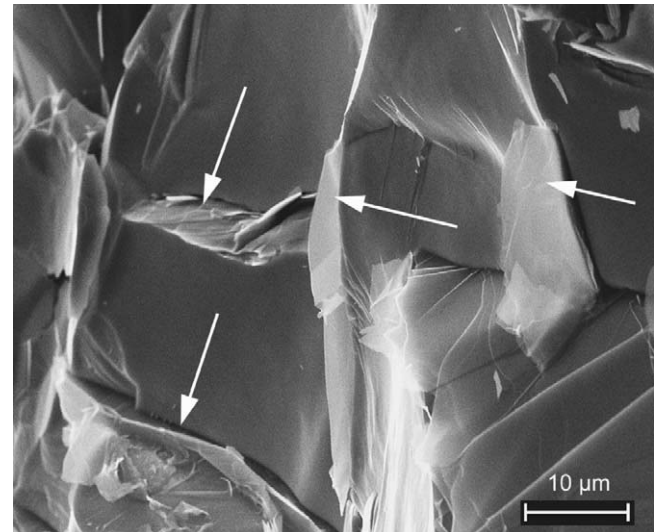

Fig. 13. Close-up of pulled-out β-WB (arrows). Note bending of laminar crystals.
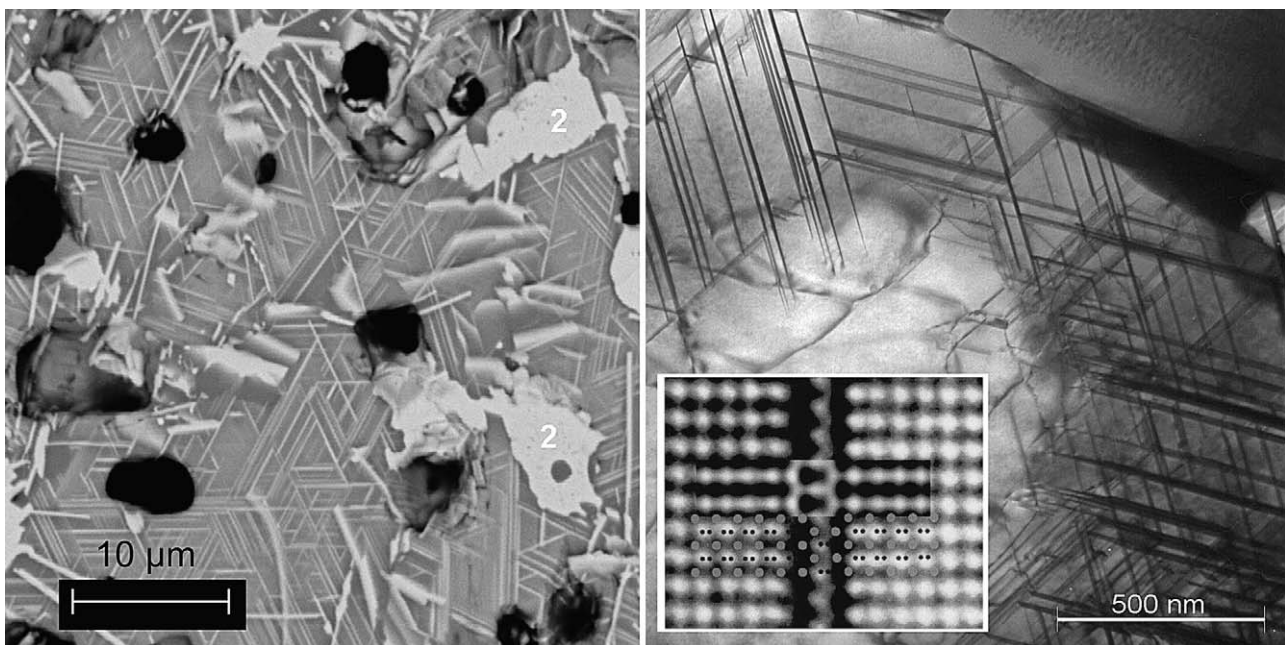

Fig. 12. Epitaxial β-WB precipitates in supersaturated $(Ti, W, Cr)B_2$ solid solutions. 2: W_2B_5. Left: SEM-image; right: TEM image with high resolution insert.
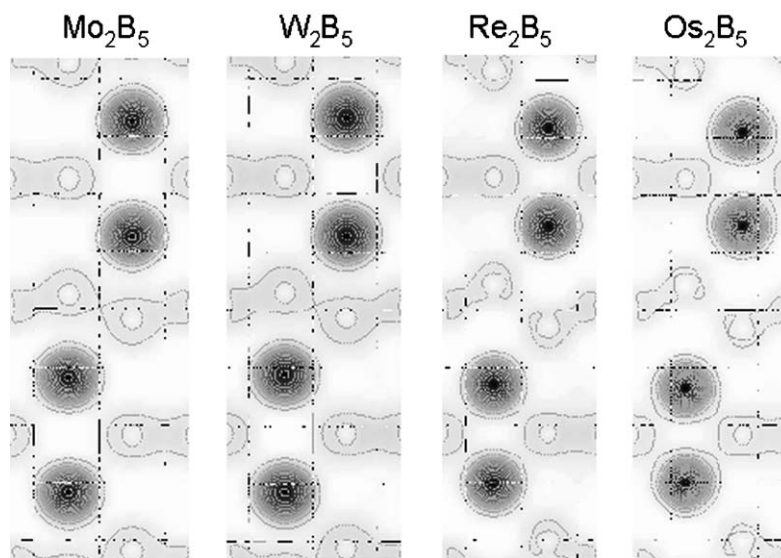
Fig. 14. Comparison of Mo, W, Re, and Os A_2B_5-type boride electron density by ab initio calculations. Note the decreasing distance between the metal atoms and progressive weakening of the interlayer bonding with increasing atomic number. Electron density increases from 0.1 (white) to 5.2 (grey) electrons/Å^3.

4. Discussion

Similar to particular ternary carbides and nitrides of layered structures there is also a group of transition metal borides which crystallise in a layered structure with weak interatomic bonding between the layers. An interesting candidate is the AlB_2-type structure and its derivatives such as W_2B_5 and Mo_2B_5, as well as the less-known Re_2B_5 and Os_2B_5 as representatives as derived from ab initio calculations. Many experiments prove, however, that the members of the AlB_2 structure type family possess exceptionally high hardness, although being anisotropic, and do not show any tendency to delamination rupture. This is more likely in structures with some additional abnormalities such as puckered boron layers or a pronounced inclination to form stacking faults thus giving easy access to foreign atoms.

In case of W_2B_5 the following observations have been made: (i) W_2B_5 crystallises preferentially in a platelet shape whether it is generated from its melt or from precipitation from liquid or solid solutions. (ii) W_2B_5 stacks may easily transform to $P6/mmm$ symmetry if other metals are incorporated in the lattice or assembled at the surface, e.g. by segregation during grain growth. (iii) W_2B_5 crystals may be easily bent elastically and deformed plastically by delamination and kink band formation although they are regarded as stiff with Young's modulus of 770 GPa and Vickers hardness of 21–26 GPa $HV_{0.05}$ [24,25].

In order to take advantage of this "nano-laminate" behaviour, W_2B_5 particles of platelet shape have been incorporated into ceramic matrices of boron carbide, silicon carbide, and titanium diboride-based composites. It can be shown on fracture surfaces that the well-known reinforcing mechanisms such as crack deflection, crack bridging, and particle pull-out are active. Depending on grain size, grain boundary strength, thermal mismatch,

etc., crack deflection is generated *inside* W_2B_5 particles rather than at the phase boundary. This is intended since it is most difficult to adjust the properties of the grain boundaries to the particular load cases applied. Furthermore, it is possible to grow these phases from supersaturated solid solutions in situ to the dimensions desired. It was shown—not reported here—that the same is possible with the structurally related Mo_2B_5 phase [26].

A comparison with studies on single phase W_2B_5 but also on single crystals, e.g. by Bulfon et al. [24] and Otani et al. [25] yields, however, no evidence that delamination has occurred upon testing hardness or Young's modulus. This may imply that in the present work, i.e. in the presence of other elements, the bonding between the layers is weakened even more. In these cases a termination of crystal growth seems to be more likely since the continuous growth of a constrained crystal is energetically less favoured. This was also suggested by [13,18], who estimated the strain arising from the stacking sequence hosting a partially occupied puckered boron layer, i.e. K′ with 4f position as the lateral extension of the relaxed boron layer is slightly less than that of the metal layer. Confirmation was given by the observation of rolling-up crystals as created by the auxiliary bath method after the metallic matrix was removed. Additionally the deformation mechanism proposed by Barsoum et al. [9,10] is obviously effective as well. Because of the ability for delamination parallel to (0001) both tensile and compressive strengths perpendicular to the c-axis are very high. This is also known from the cases of graphite and most of the layered silicates such as chrysotile. This consideration is supported by elemental analysis showing that considerable quantities of, e.g., TiB_2 (max. 4 mol% at 2230 °C) and CrB_2 (max. 11 mol% at 2030 °C) are dissolved in the structure giving rise for AlB_2-type stacking faults [13,14]. In the case of

Mo_2B_5 similar phenomena have been observed, too, but the quantification of the effects is still in progress. Furthermore, the similarity in deformation behaviour of W_2B_5 and Mo_2B_5 with MAX-phases is consistent with the ab initio data presented here: The electron density distributions in $(11\bar{2}0)$ planes for the Mo, W, Re, and Os A_2B_5-type borides are rather similar to the electron density distributions in $(11\bar{2}0)$ planes of MAX-phases, see for example [27,28]. Hence, it is evident that the chemical bond in $(11\bar{2}0)$ planes is rather similar. Therefore it is not surprising that W_2B_5-based compounds exhibit similar properties to MAX-phases.

Surprisingly, another phase being precipitated from $(Ti, W, Cr)B_2$ solid solutions also shows nano-laminate behaviour: β-WB. It could not be expected that crystals only some nanometres thick might withstand crack propagation perpendicular to the platelet plane. Moreover, debonding from the surrounding host crystal was not likely to occur very easily because of the structural similarity with the matrix [14].

5. Conclusion

Besides carbon and nitrogen-based MAX-phases there is a group of unexplored transition metal borides which exhibit the rather unique behaviour of "nano-lamination". Ab initio data suggests that the bonding in the in $(11\bar{2}0)$ planes of MAX-phases and the investigated transition metal borides is rather similar. It is proved that these materials act as reinforcing compounds in brittle ceramic and metallic matrices providing *intracrystalline* crack deflection, crack bridging, and particle pull-out. Since these phases tend to form platelet-shaped particles grown in situ either by precipitation from supersaturated solid solutions or by heterogeneous nucleation at grain boundaries there is no need for a powder metallurgical processing considered most difficult to obtain a homogeneous distribution and full density. Furthermore, grain size and c/a-ratio of the platelets may be controlled by means of annealing temperature and time. Thus, transition metal borides, "TMB", should be regarded as an interesting type of nano-laminates.

Acknowledgment

References

[1] W. Jeitschko, H. Nowotny, Monatsh. Chem. 98 (1967) 329–337.
[2] H. Wolfsgruber, H. Nowotny, F. Benesovsky, Monatsh. Chem. 98 (1967) 2401.
[3] H. Nowotny, Prog. Solid State Chem. (1970) 27.
[4] M.A. Pietzka, J.C. Schuster, J. Phase Equilib. 15 (1994) 392–400.
[5] M.W. Barsoum, D. Brodkin, T. El-Raghy, Scr. Met. Mater. 36 (1997) 535–541.
[6] M.W. Barsoum, T. El-Raghy, Met. Mater. Trans. 30A (1999) 363–369.
[7] M.W. Barsoum, M. Ali, T. El-Raghy, Met. Mater. Trans. 31A (2000) 1857–1865.
[8] M.W. Barsoum, T. El-Raghy, Am. Sci. 89 (2001) 336–345.
[9] M.W. Barsoum, T. Zhen, S. Kalindini, M. Radovic, A. Murugaiah, Nat. Mater. 2 (2003) 107–111.
[10] M.W. Barsoum, M. Radovic, in: Encyclopedia of Materials: Science and Technology, Elsevier, The Netherlands, 2004, pp. 1–16.
[11] D.R. Armstrong, in: H. Werheit (Ed.), Proceedings of the Nineth International Symposium on Boron, Borides, and Related Compounds, Duisburg, Germany, September 21–25 1987, University Press, Duisburg, 1987, pp. 125–131.
[12] E. Fendler, O. Babushkin, T. Lindbäck, R. Telle, G. Petzow, J. Hard Mater. (4) (1993) 137–148.
[13] A. Pohl, R. Telle, G. Petzow, Z. Metallkunde 86 (2) (1995) 148–151.
[14] W. Mader, B. Freitag, K. Kelm, R. Telle, C. Schmalzried (Eds.) Mater. Res. Symp. Proc. vol. 589, Mater. Res. Soc. (2001) 289–294.
[15] P. Hohenberg, W. Kohn, Phys. Rev. 136 (1964) B864.
[16] G. Kresse, D. Joubert, Phys. Rev. B 59 (1999) 1758.
[17] A. Pohl, Untersuchungen zum Kristallwachstum der Übergangsmetallboride TiB_2, W_2B_5 und deren Mischkristalle zur Verstärkung keramischer Matrizes, Ph. D. Thesis, University of Stuttgart, Germany, 1993, 138pp.
[18] R. Telle, A. Pohl, Jpn. J. Appl. Phys. Ser. 10, R. Uno, I. Higashi (Eds.), Publication Office, Jpn. J. Appl. Phys., Tokyo, 1994, pp. 194–197.
[19] R. Telle, Ceramics for High-tech Applications, Material Science, European Concerted Action COST 503 Powder Metallurgy—Powder Based Materials, vol. V, T. Valente, Directorate-General, Science, Research and Development, Brussels, 1997, 296pp.
[20] R. Telle, C. Schmalzried, Z. Metallkunde 92 (11) (2001) 1197–1202.
[21] C.P. Kempter, et al., J. Chem. Phys. 34 (1961) 1994.
[22] Z. Sun, D. Music, R. Ahuja, S. Li, J.M. Schneider, Phys. Rev. B 70 (2004) 092102.
[23] M.W. Barsoum, Prog. Solid. State Chem. 28 (2000) 201.
[24] C. Bulfon, A. Leithe-Jasper, H. Sassik, P. Rogl, in: Materialwissenschaftliche Grundlagen, Symposium 7, Proceedings of the Werkstoffwoche'96, Stuttgart, 1996, 1997, pp. 191–196.
[25] S. Otani, H. Ohashi, Y. Ishizawa, J. Alloys Compds. 221 (1995) L8–L10.
[26] C. Schmalzried, R. Telle, Project No. 03N8616A, Federal Ministry of Education and Research (BMBF) of the Federal Republic of Germany, Final Report, 2001.
[27] Z. Sun, D. Music, R. Ahuja, S. Li, J.M. Schneider, Phys. Rev. B 70 (2004) 092102.
[28] Z. Sun, D. Music, R. Ahuja, J.M. Schneider, Phys. Rev. B 71 (2005) 193402.